PNAS

Supporting Information for

Chondroitin 4-*O*-sulfation regulates hippocampal perineuronal nets and social memory

Huiqian Huang, Amélie M. Joffrin, Yuan Zhao, Gregory M. Miller, Grace C. Zhang, Yuki Oka, Linda C. Hsieh-Wilson*

*Correspondence: Linda C. Hsieh-Wilson
Email: lhw@caltech.edu

This PDF file includes:

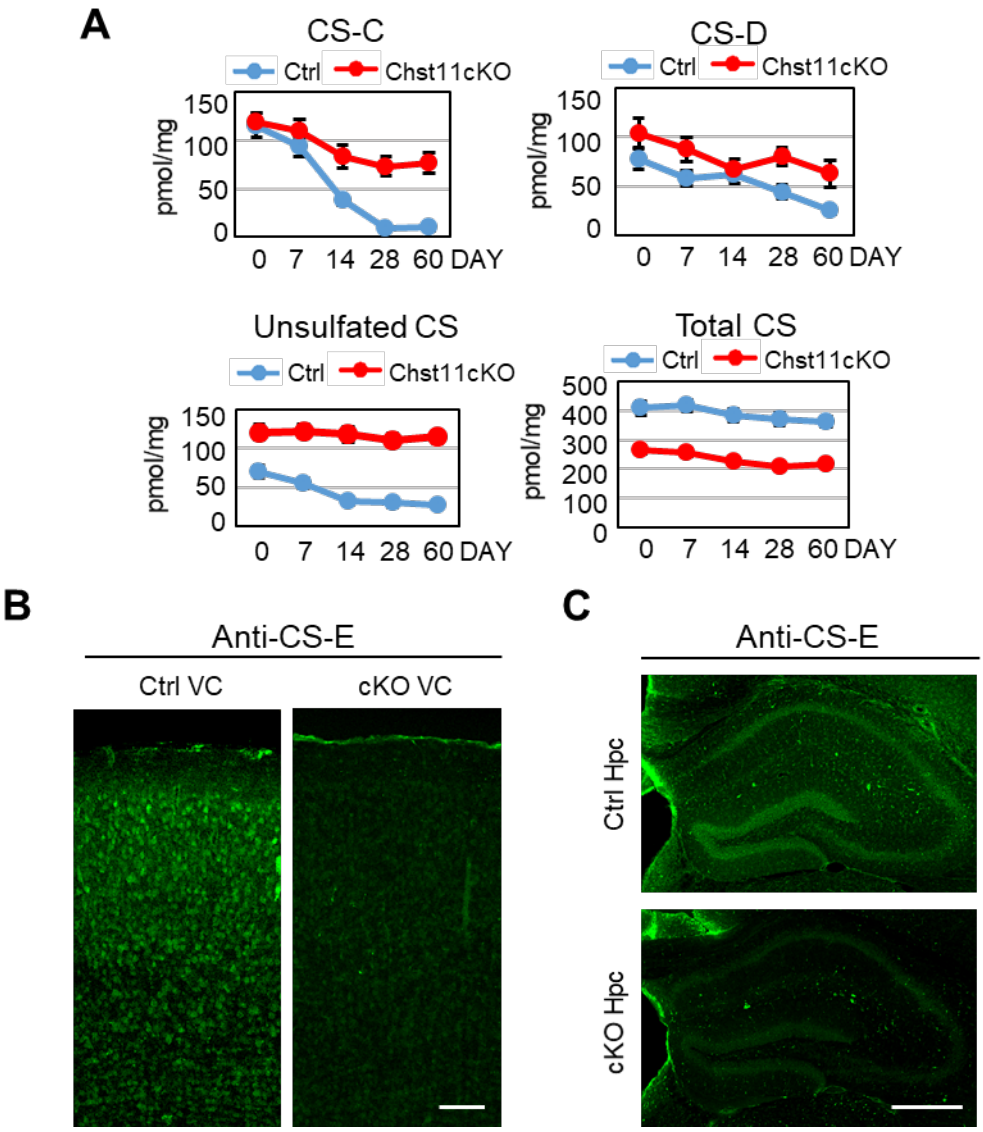

Figure S1. Disruption of the 4-*O*-sulfation pathway in Chst11cKO mice. (**A**) HPLC disaccharide analysis was used to quantify the amounts of CS-C, CS-D, unsulfated CS and total CS in the cortex of Ctrl (blue) and Chst11cKO (red) mice at postnatal day (P) 0, P7, P14, P28 and P60. The amounts were calculated by dividing the number of picomoles (pmol) of CS by the total weight (mg) of the dried homogenate. (**B**) Representative images of brain slices showing the visual cortex (VC) of Ctrl and Chst11cKO mice immunostained with an anti-CS-E monoclonal antibody. Scale bars, 100 μm. (**C**) Representative images of brain slices showing the hippocampus (Hpc) of Ctrl and Chst11cKO mice immunostained with a CS-E monoclonal antibody. Scale bars, 500 μm.

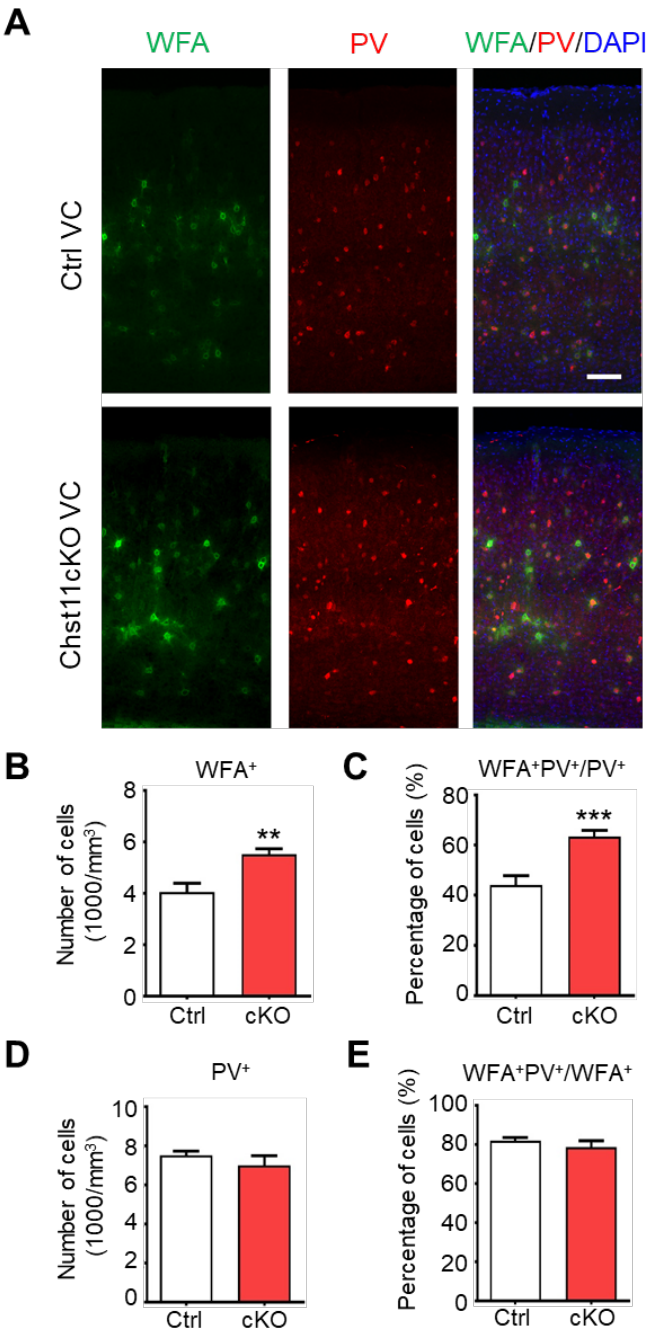

Figure S2. Increased PNN densities in the VC of Chst11cKO mice. (**A**) Representative images showing PNN-enwrapped (WFA^+) and parvalbumin-expressing (PV^+) neurons in the VC of Ctrl and Chst11cKO mice. Brain sections were stained with WFA (green), an anti-parvalbumin antibody (red), and DAPI (blue). Scale bar, 100 µm. (**B**) Quantification of the number of WFA^+ neurons in the VC. $^{**}P < 0.01$ vs. Ctrl, Student's *t*-test. (**C**) Percentage of WFA^+ PV^+ neurons amongst the PV^+ neurons. $^{***}P < 0.001$ vs. Ctrl, Student's *t*-test. (**D**) Quantification of the number of PV^+ neurons in the VC. Not significant. (**E**) Percentage of WFA^+ PV^+ neurons amongst the WFA^+ neurons. Not significant. *n* = 14 brain slices each from 4 pairs of Ctrl and Chst11cKO mice for **B**-**E**. All data are shown as the mean ± SEM.

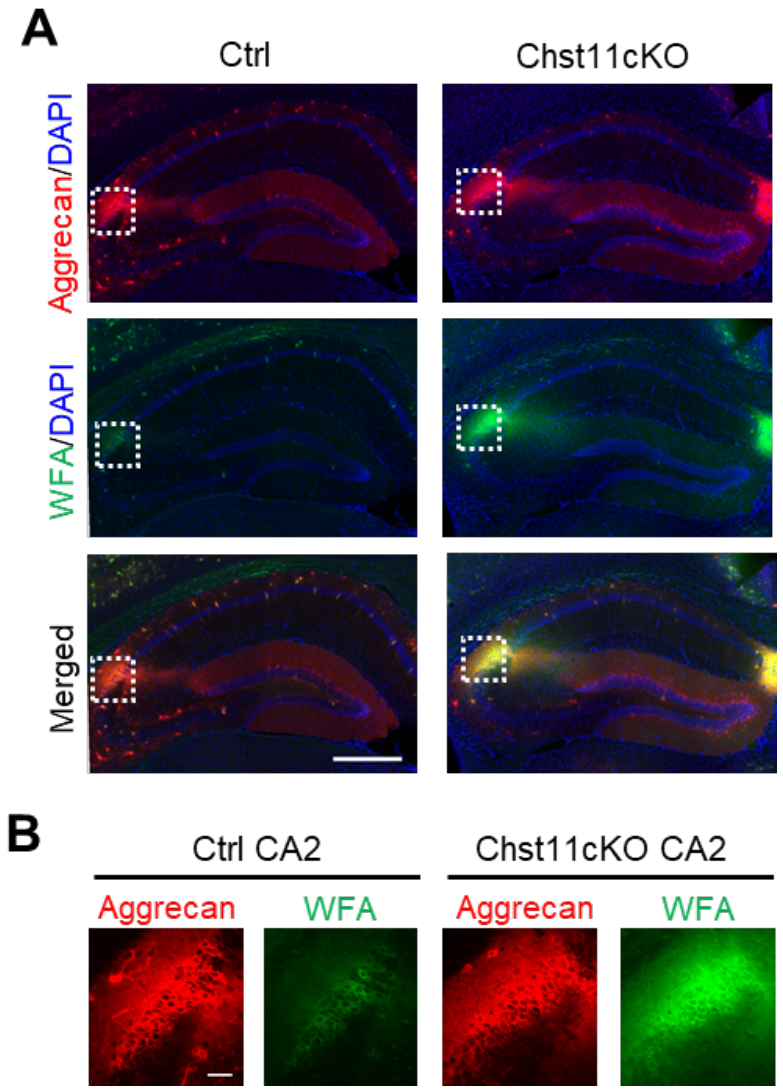

Figure S3. Comparable aggrecan levels in the CA2 regions of Ctrl and Chst11cKO mice. (**A**) Representative images showing PNN and aggrecan staining in the hippocampus of Ctrl and Chst11cKO mice. Brain sections were stained with WFA (green), an anti-aggrecan antibody (red), and DAPI (blue). The CA2 regions are marked with dotted white squares. Scale bar, 500 μm. *n* = 3 pairs each of Ctrl and Chst11cKO mice. (**B**) Magnified images showing the PNN-enriched CA2 regions of Ctrl and Chst11cKO mice, stained for aggrecan (red) and PNNs (WFA, green). Scale bar, 50 μm.

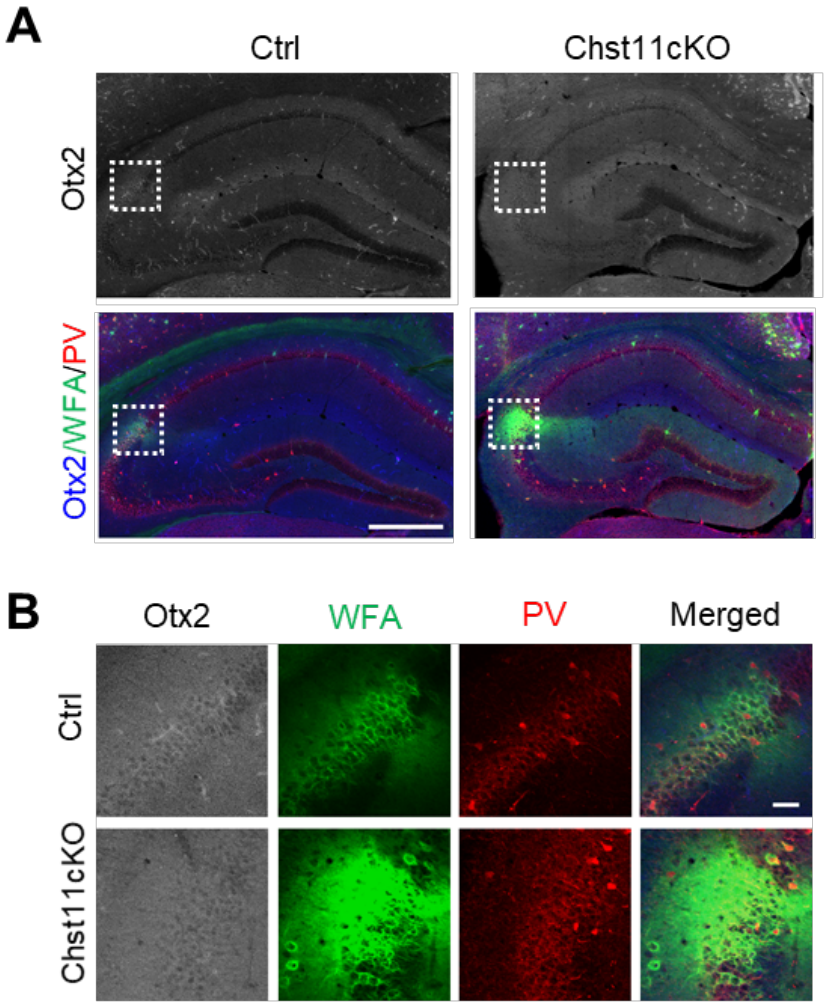

Figure S4. Low, comparable levels of Otx2 in the CA2 regions of Ctrl and Chst11cKO mice. (**A**) Representative images showing PNN and Otx2 staining in the hippocampus of Ctrl and Chst11cKO mice. Brain sections were stained with WFA (green), an anti-parvalbumin antibody (red), and an anti-Otx2 antibody (grey in separate images; blue in merged images). CA2 regions are marked with dotted white squares. Scale bar, 500 μm. *n* = 2 pairs each of Ctrl and Chst11cKO mice. (**B**) Magnified images showing the PNN-enriched CA2 regions of Ctrl and Chst11cKO mice, stained for Otx2 (grey scale), PNNs (WFA, green), and PV (red). Scale bar, 50 μm.

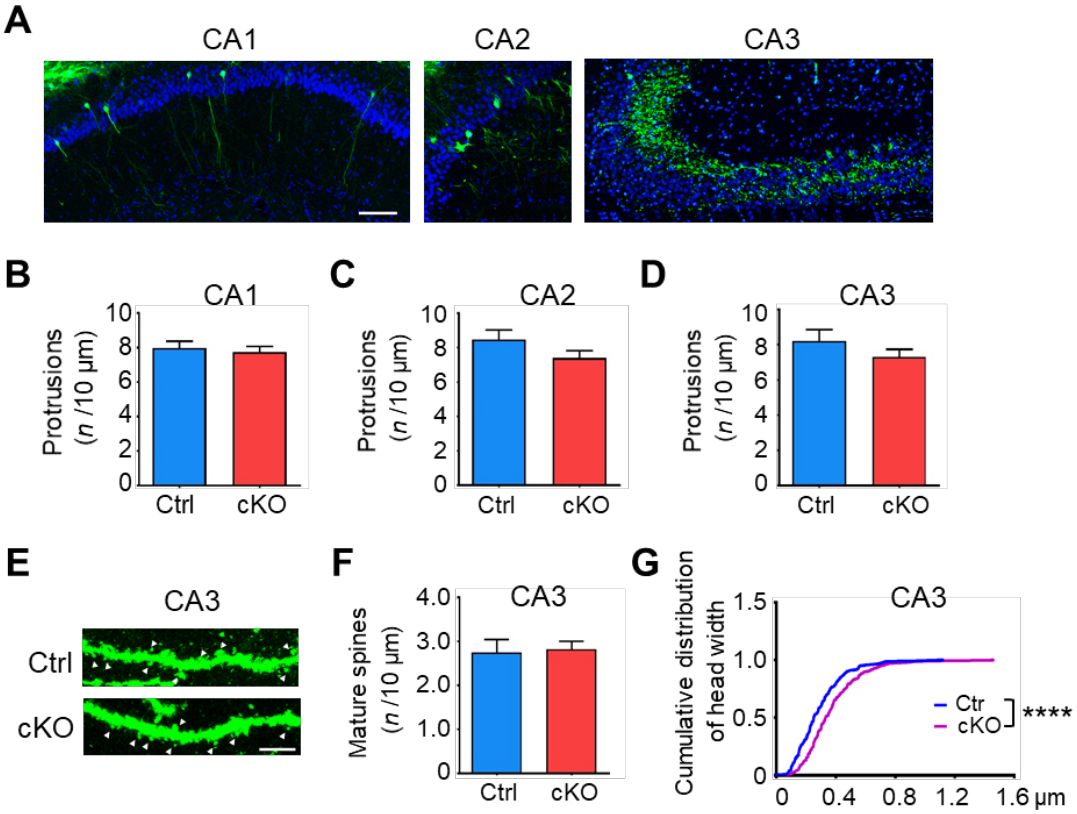

Figure S5. Dendritic spine morphology of hippocampal neurons in Ctrl and Chst11cKO mice. (**A**) Representative images showing the hippocampal CA1, CA2, and CA3 regions of Ctrl mice injected with GFP-expressing lentivirus. Scale bar, 100 μm. (**B** to **D**) No significant difference was observed in the protrusion densities in the CA1 (**B**), CA2 (**C**), and CA3 (**D**) regions of Chst11cKO mice compared to Ctrl mice. Not significant; n = 23, 22 dendrites in the CA1, n = 13, 16 dendrites in the CA2, and n = 11, 15 dendrites in the CA3 regions of Ctrl and Chst11cKO mice, respectively. Data are shown as the mean ± SEM. (**E** to **G**) CA3 neurons from Chst11cKO mice have larger dendritic spine head widths, but similar mature spine density. Representative images of the dendritic spines from GFP-expressing CA3 neurons are shown in **E**. Scale bar, 5 μm. Quantification of the mature spine density is shown in **F**. Not significant; n = 11 and 15 dendrites from 3 pairs of Ctrl and Chst11cKO mice, respectively. Data are shown as the mean ± SEM. Cumulative distribution curves of spine head width for Ctrl and Chst11cKO CA3 neurons are shown in **G**. ****P < 0.0001 vs. Ctrl, Kolmogorov–Smirnov test.

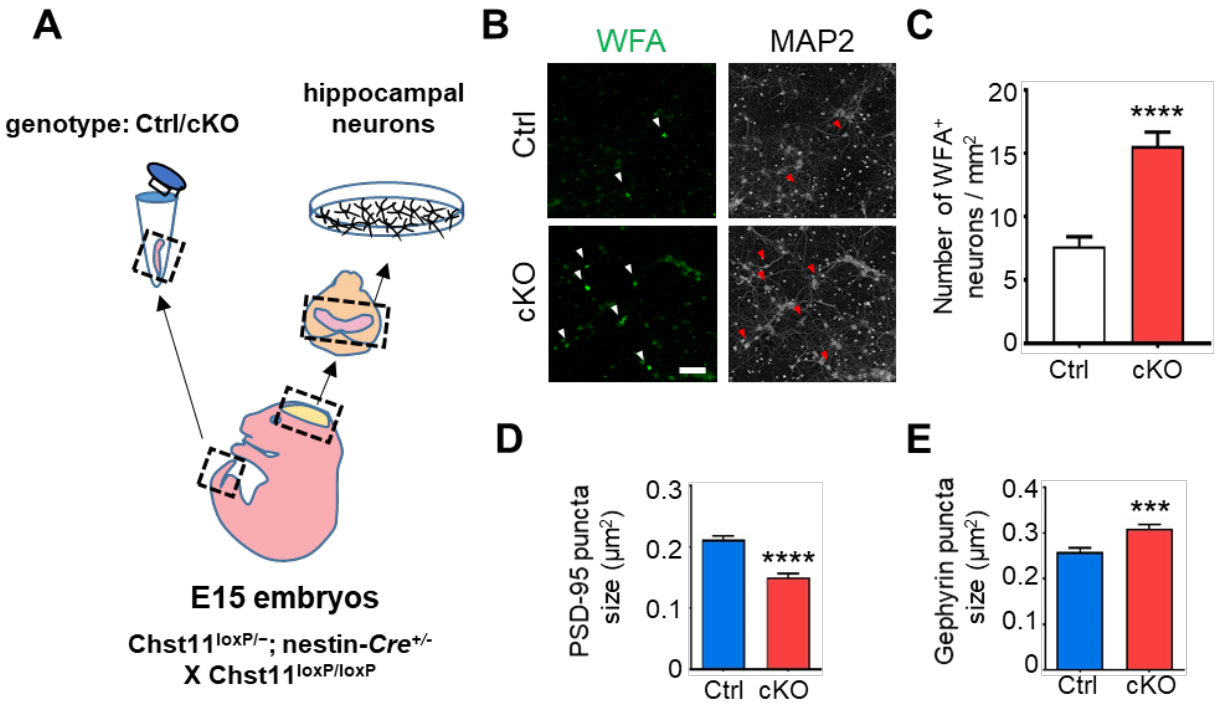

Figure S6. Altered PNN densities and synapse sizes in cultured hippocampal Chst11cKO neurons compared to Ctrl neurons. (**A**) Schematic showing the collection and culturing of hippocampal neurons from individual embryos at embryonic day 15 (E15). The tail of each embryo was collected for genotyping. (**B**) Representative images showing hippocampal neuron cultures from Ctrl and Chst11cKO embryos stained with WFA (green) and an anti-MAP2 antibody (grey scale). The same PNN$^+$ neurons were indicated with white or red arrowheads in separate channels for WFA or MAP2, respectively. Scale bar, 100 μm. (**C**) Quantification of the number of WFA$^+$ neurons per mm^2. ****P < 0.0001 vs. Ctrl, Student's t-test; n = 22 and 21 regions of cultured neurons from 3 pairs of Ctrl and Chst11cKO mice, respectively. (**D**) Quantification of PSD-95 puncta size. ****P < 0.0001 vs. Ctrl, Student's t-test; n = 20 neurons each for Ctrl and Chst11cKO mice. (**E**) Quantification of gephyrin puncta size. ***P < 0.001 vs. Ctrl, Student's t-test; n = 20 neurons each for Ctrl and Chst11cKO mice. All data are shown as the mean ± SEM.

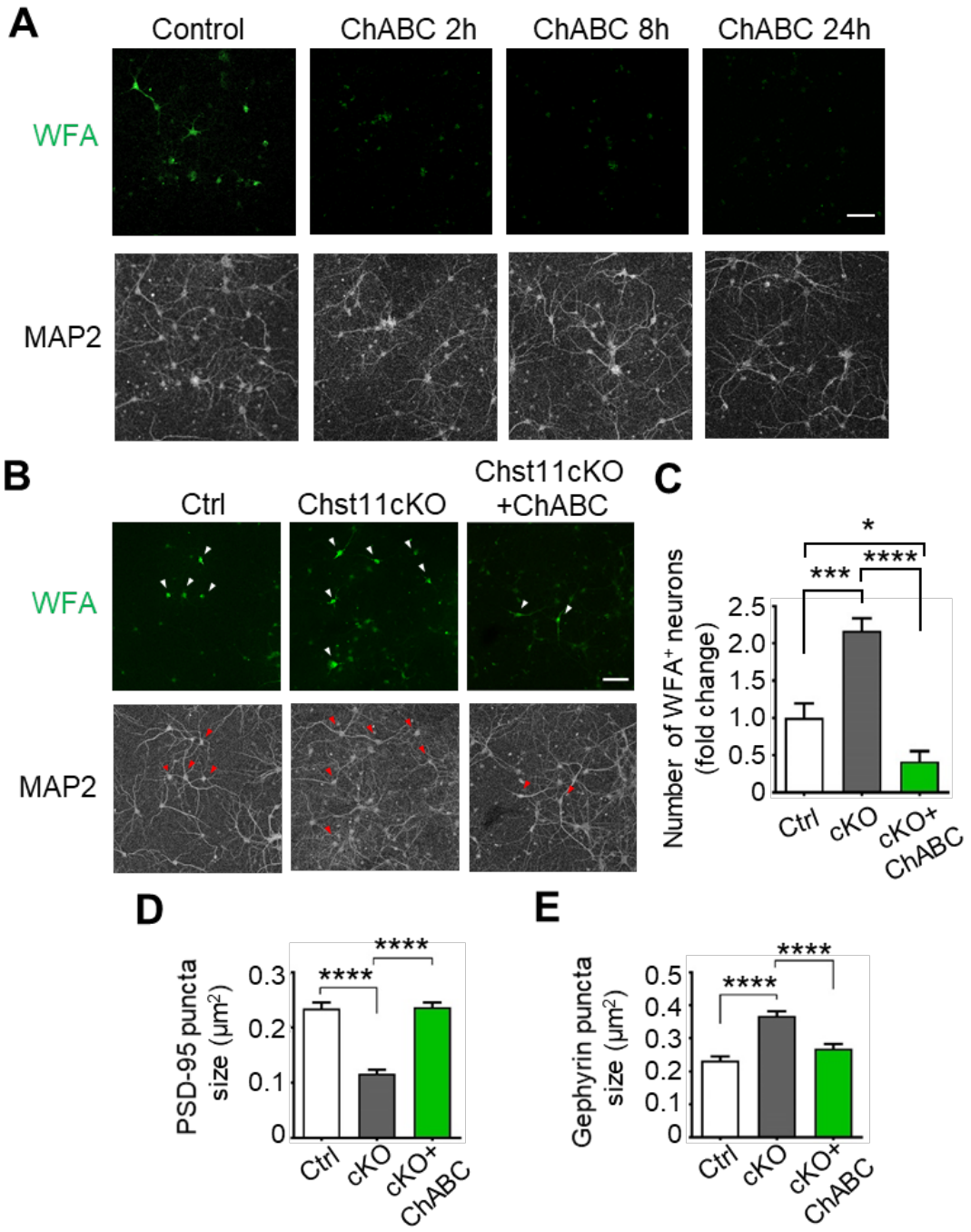

Figure S7. ChABC treatment of cultured Chst11cKO neurons removes excess PNNs and restores synapse sizes to Ctrl neuron levels. (**A**) Representative images showing wild-type C57 hippocampal neurons treated with PBS (Control) or ChABC for 2, 8, or 24 h, and stained for PNNs (WFA, green) and MAP2 (grey scale). Scale bar, 100 μm. (**B**) Representative images of Ctrl, Chst11cKO, and ChABC-treated Chst11cKO cultured hippocampal neurons stained for PNNs (WFA, green) and MAP2 (grey scale). The same PNN$^+$ neurons were indicated with white or red arrow heads in separate channels for WFA or MAP2, respectively. Scale bar, 100 μm. (**C**) Quantification of the number of WFA$^+$ neurons in each visual field, normalized to Ctrl. *P < 0.05, ***P < 0.001, ****P < 0.0001 vs. Ctrl, one-way ANOVA followed by Tukey's multiple comparisons test; n = 6, 6, and 8 regions of Ctrl, Chst11cKO, and ChABC-treated Chst11cKO cultured neurons, respectively. (**D**) ChABC treatment of Chst11cKO neurons restored the PSD-95 puncta size to Ctrl

neuron levels. ****$P < 0.0001$ vs. Ctrl, one-way ANOVA followed by Tukey's multiple comparisons test; $n = 10$, 11, and 10 Ctrl, Chst11cKO, and ChABC-treated Chst11cKO cultured neurons, respectively. (**E**) ChABC treatment of Chst11cKO neurons restored the gephyrin puncta size to Ctrl neuron levels. ****$P < 0.0001$ vs. Ctrl, one-way ANOVA followed by Tukey's multiple comparisons test; $n = 10$ neurons for each condition. All data are shown as the mean ± SEM.

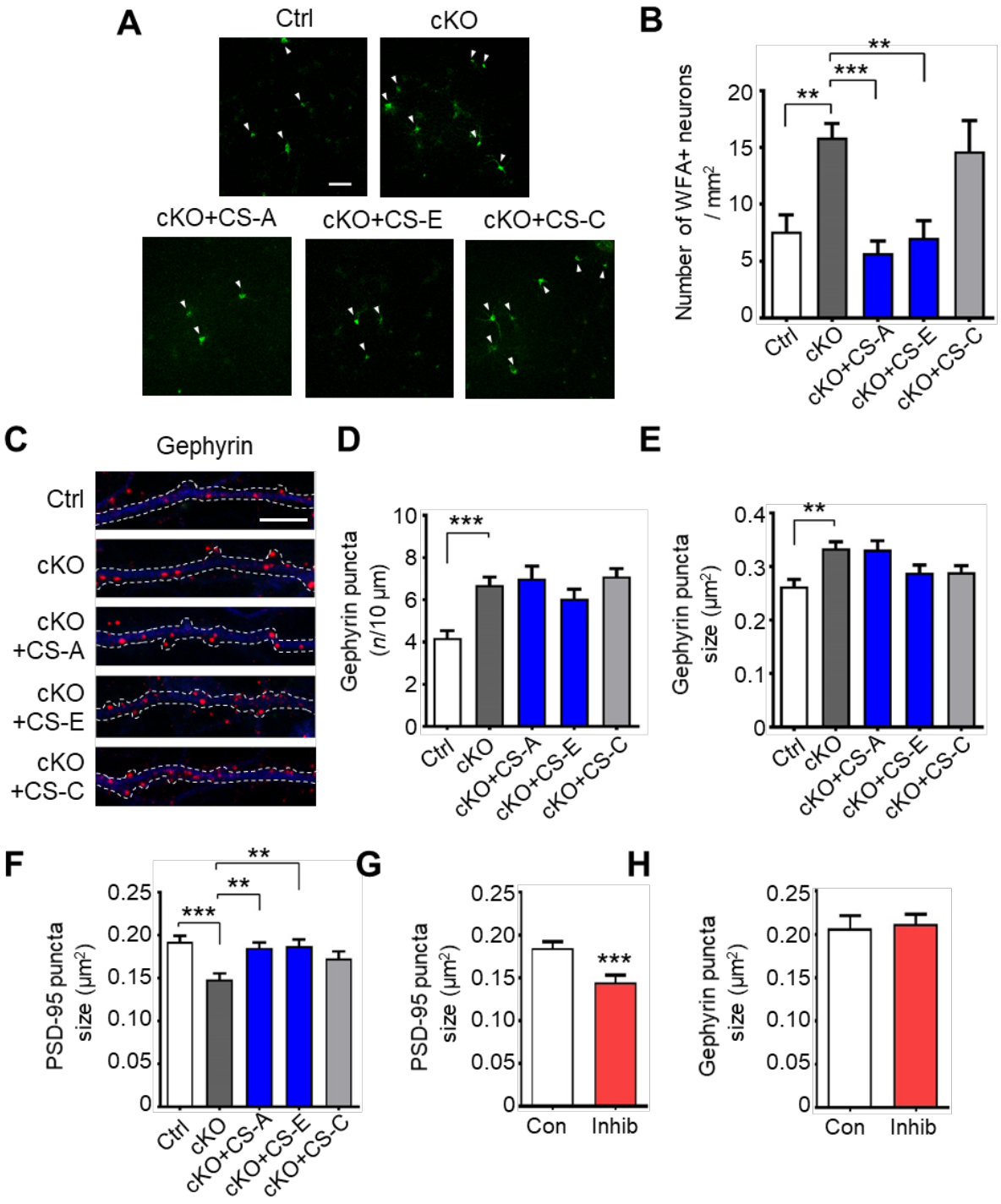

Figure S8. Chemical manipulation of CS 4-*O*-sulfation levels modulates PNN densities and synapses. (**A** and **B**) Treatment of Chst11cKO neurons (13–15 DIV) with natural CS polysaccharides (20 µg/ml) enriched in the 4-*O*-sulfated CS-A or CS-E motifs, but not the 6-*O*-sulfated CS-C motif, restored PNN densities to Ctrl neuron levels. Representative images of hippocampal neuronal cultures for the conditions indicated are shown in **A**. Scale bar, 100 µm. Quantification of the number of WFA^+ neurons per mm^2 is shown in **B**. $^{**}P < 0.01$, $^{***}P < 0.001$ vs. Chst11cKO, one-way ANOVA followed by Tukey's multiple comparisons test; n = 9, 8, 9, 9, and 9 regions of Ctrl, Chst11cKO, and CS-A, CS-E or CS-C-treated Chst11cKO cultured neurons,

respectively. (**C** to **E**) Addition of natural CS polysaccharides to cultured Chst11cKO hippocampal neurons did not rescue the increased density or size of gephyrin puncta. Representative images of gephyrin puncta (red) distributed along the dendrites of neurons (MAP2, blue) cultured under the indicated conditions are shown in **C**. Scale bar, 10 μm. Quantification of gephyrin puncta number per 10 μm (**D**) and size (**E**). $^{**}P < 0.01$, $^{***}P < 0.001$ vs. Chst11cKO, one-way ANOVA followed by Tukey's multiple comparisons test; n = 10, 12, 10, 10, and 10 for Ctrl, Chst11cKO, and CS-A, CS-E or CS-C-treated Chst11cKO neurons, respectively. (**F**) Addition of natural CS polysaccharides enriched in the CS-A or CS-E motifs, but not the CS-C motif, rescued the decreased size of PSD-95 puncta in Chst11cKO neurons. Quantification shows PSD-95 puncta size. $^{**}P < 0.01$, $^{***}P < 0.001$ vs. Chst11cKO, one-way ANOVA followed by Tukey's multiple comparisons test; n = 15, 13, 14, 10, and 12 neurons for Ctrl, Chst11cKO, and Chst11cKO neurons treated with CS-A, CS-E or CS-C, respectively. (**G**) Treatment with a sulfotransferase inhibitor (Inhib, 10 μM, 24 h) reduced the PSD-95 puncta size. Quantification of PSD-95 puncta size. $^{***}P < 0.001$ vs. Con, Student's t-test; n = 10 and 9 neurons treated with Inhib in DMSO or DMSO alone (Con), respectively. (**H**) Inhib treatment (10 μM, 24 h) did not change the gephyrin puncta size. Quantification of gephyrin puncta size. n = 9 and 8 neurons treated with Inhib in DMSO or DMSO alone (Con), respectively. All data are shown as the mean ± SEM.

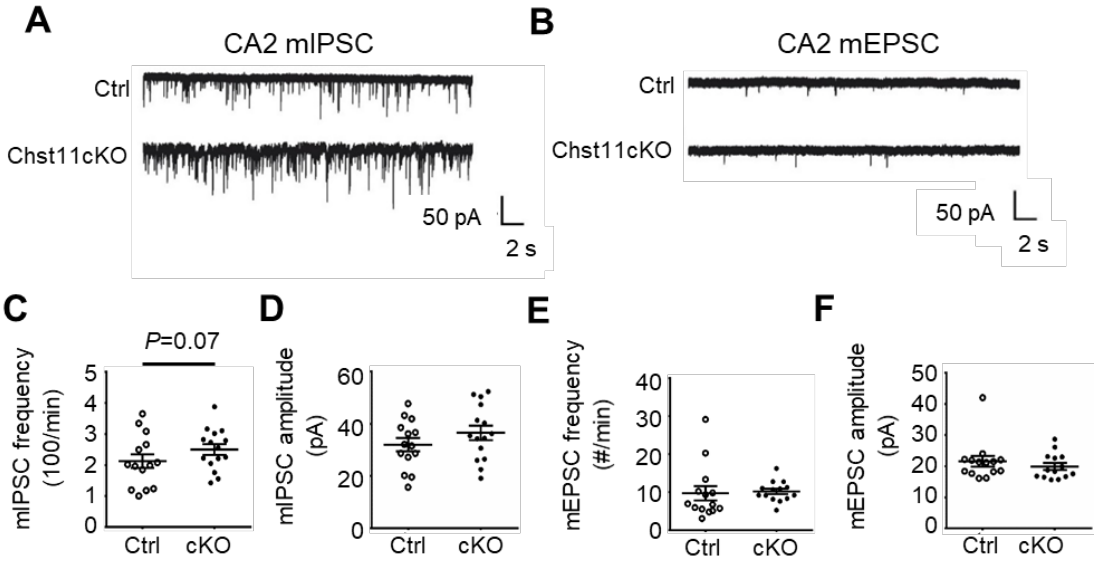

Figure S9. mIPSC and mEPSC recordings of CA2 neurons from Ctrl and Chst11cKO mice. (**A and B**) Raw traces of mIPSC (**A**) and mEPSC (**B**) of CA2 neurons from Ctrl and Chst11cKO mice. (**C** and **D**) Quantification revealed that mIPSC frequency (**C**) for Chst11cKO CA2 neurons showed an increasing trend compared to Ctrl CA2 neurons. *P* = 0.07, Wilcoxon rank-sum one-sided test. The mIPSC amplitude (**D**) was not significantly different between Ctrl and Chst11cKO neurons; *n* = 14 and 15 neurons from 3 Ctrl and 5 Chst11cKO mice, respectively. (**E** and **F**) mEPSC frequency (**E**) and amplitude (**F**) were comparable for Ctrl and Chst11cKO CA2 neurons. Not significant; *n* = 14 neurons each from 4 Ctrl and 6 Chst11cKO mice. All data are shown as the mean ± SEM.

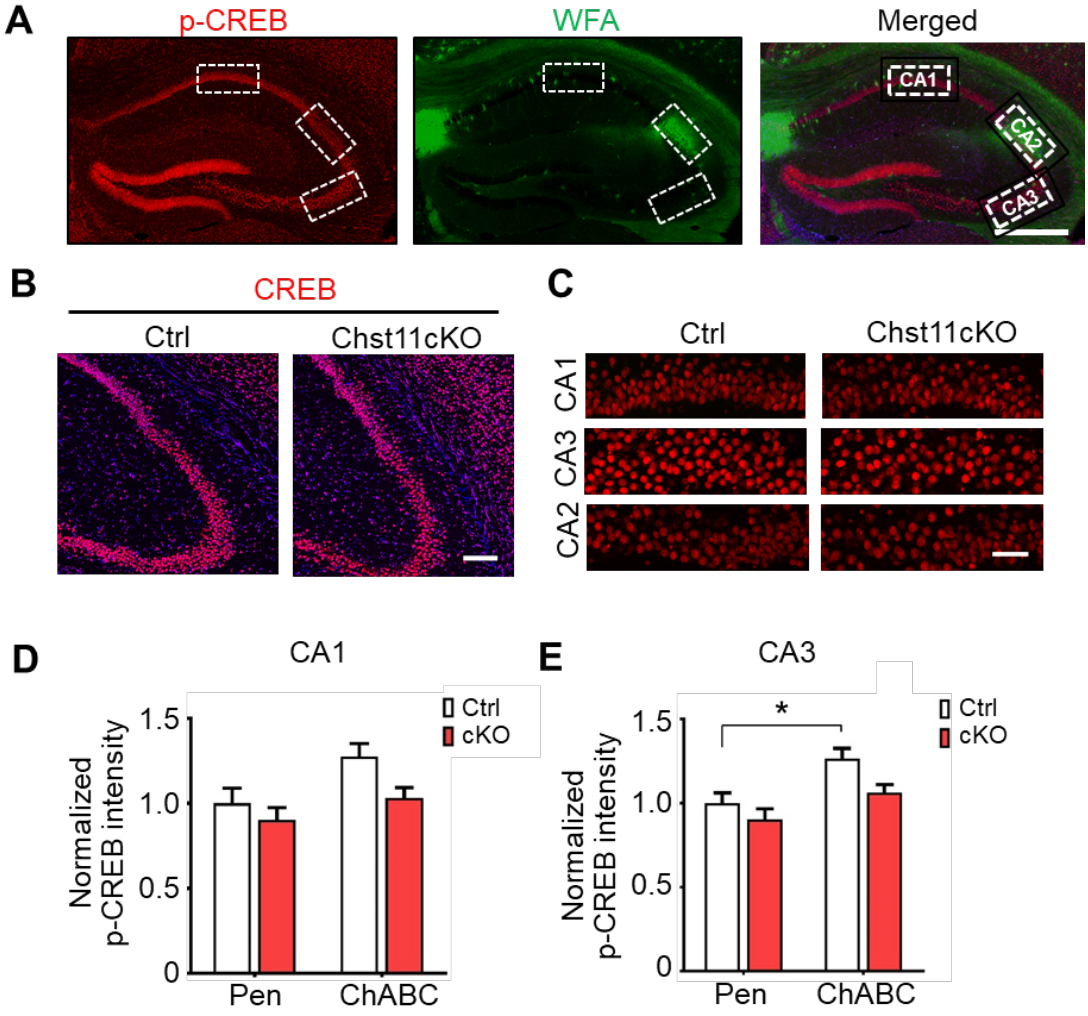

Figure S10. PNN densities modulate CREB phosphorylation levels, but not total CREB levels, in the hippocampus. (**A**) Representative images showing the CA1, CA2, and CA3 regions of the hippocampus stained with a p-CREB antibody (red) and WFA (green). Each region was cropped with a rectangular box, as indicated, for analysis of p-CREB levels at the cellular level. Scale bar, 500 μm. (**B**) Representative images showing the CA2 and CA3 hippocampal regions of Ctrl and Chst11cKO mice immunostained for CREB (red). Scale bar, 200 μm. (**C**) Representative images of cropped CA1, CA2, and CA3 regions of total CREB. Scale bar, 50 μm. (**D** and **E**) Quantification of the average p-CREB fluorescence intensity per neuron (normalized to Ctrl Pen) in the hippocampal CA1 (**D**) and CA3 (**E**) regions of Ctrl and Chst11cKO mice, injected with ChABC or penicillinase (Pen). *P < 0.05, two-way ANOVA, F(1,33) = 0.7723, P = 0.3859 for CA3; n = 10, 9, 9, and 9 slices from 3 mice each for Ctrl Con, Ctrl ChABC, Chst11cKO Con, and Chst11cKO ChABC conditions, respectively. All data are shown as the mean ± SEM.

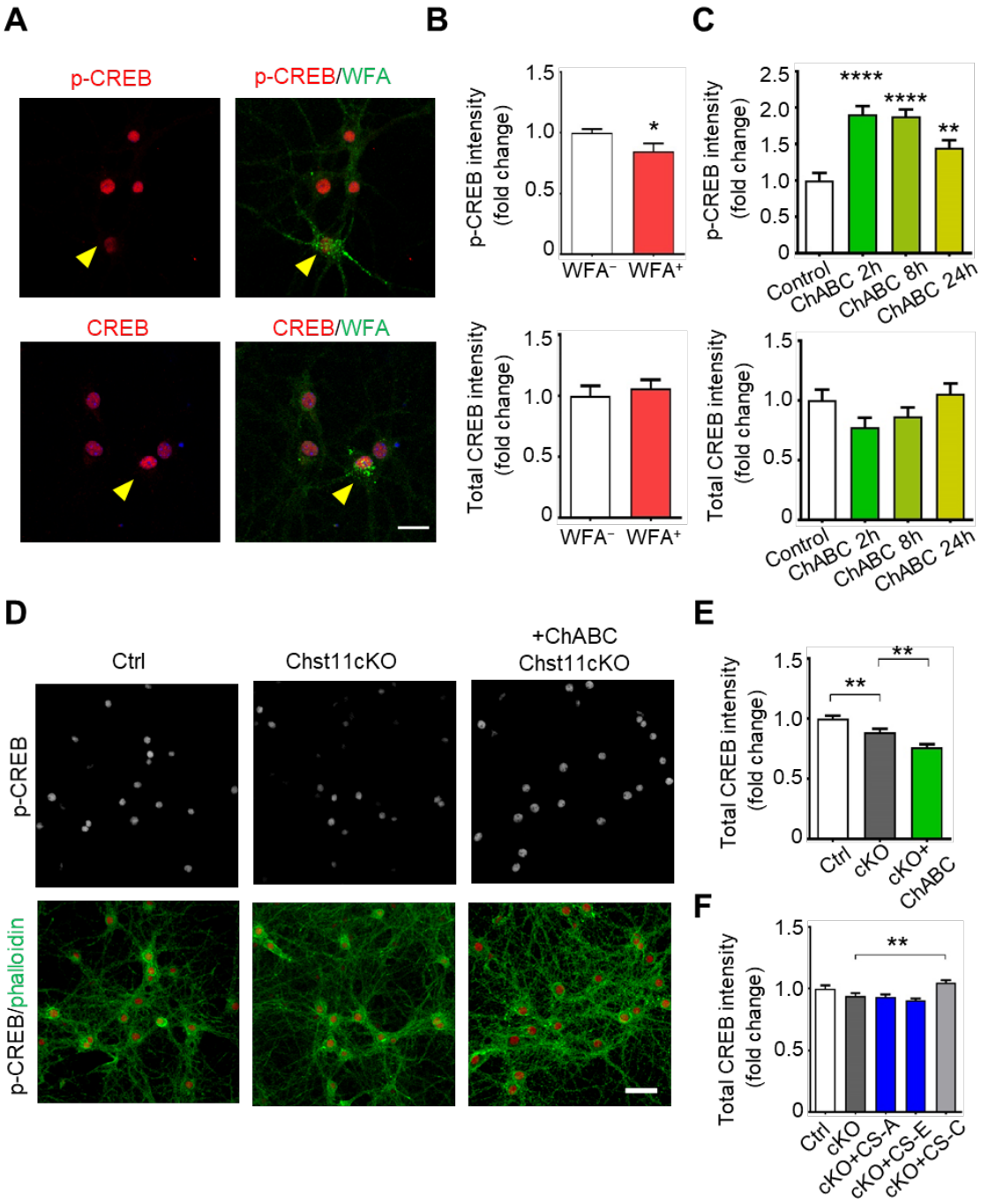

Figure S11. Modulation of PNN density and CS 4-O sulfation levels affects p-CREB levels in hippocampal neurons. (**A**) Representative images of cultured hippocampal neurons stained with WFA (green) and anti-p-CREB or anti-CREB antibodies (red) as indicated. WFA$^+$ neurons are marked with a yellow arrowhead. Scale bar, 25 μm. (**B**) Quantification of p-CREB and CREB intensities, normalized to WFA$^-$ as a control. *P < 0.05 vs. WFA$^-$, Student's t-test; n = 11 and 8 individual WFA$^-$ and WFA$^+$ neurons stained with p-CREB, respectively; n = 8 and 5 individual WFA$^-$ and WFA$^+$ neurons stained for CREB, respectively. (**C**) Quantification of p-CREB and CREB intensities in neurons treated with ChABC for 2, 8 and 24 h. **P < 0.01, ****P < 0.0001 vs. Con, one-way ANOVA followed by Tukey's multiple comparisons test; n = 100–150 neurons for each condition. (**D**) Representative images showing Ctrl and Chst11cKO hippocampal neurons treated

with ChABC or PBS as a control and stained with an anti-p-CREB antibody (upper panels, grey scale; lower panels, red) and AF488 phalloidin (green). Scale bar, 50 μm. (**E**) Quantification of total CREB levels for Ctrl, Chst11cKO, and ChABC-treated Chst11cKO neurons (normalized to Ctrl). $^{**}P < 0.01$ vs. Chst11cKO, one-way ANOVA followed by Tukey's multiple comparisons test; n = 100–150 neurons for each condition. (**F**) Quantification of total CREB levels for Ctrl, Chst11cKO, and CS-A-, CS-E- and CS-C-treated (20 μg/ml, 24 h) Chst11cKO neurons, respectively. $^{**}P < 0.01$ vs. Chst11cKO, one-way ANOVA followed by Tukey's multiple comparisons test; n = ~100–150 neurons for each condition. All data are shown as the mean ± SEM.

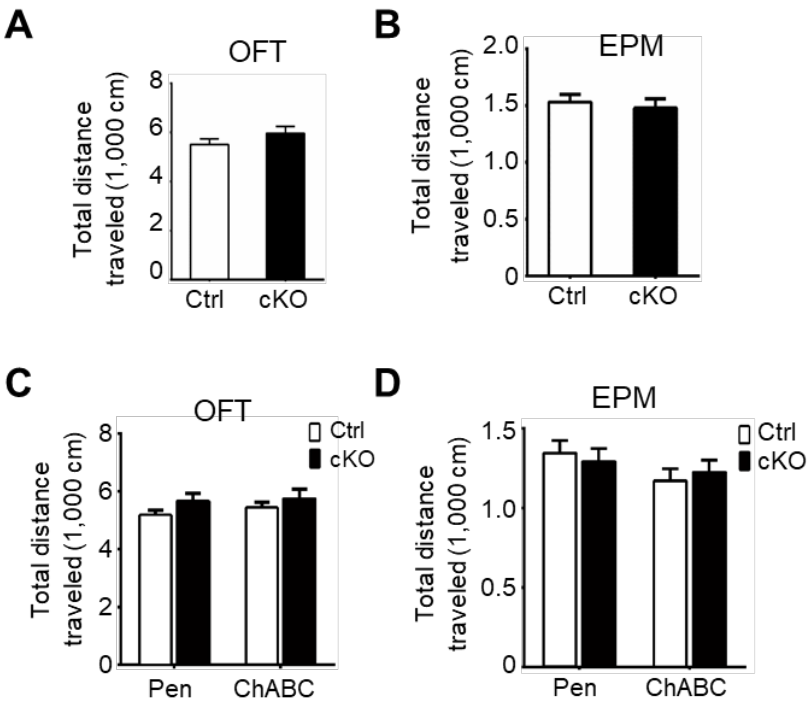

Figure S12. Locomotor activity of Ctrl and Chst11cKO mice is comparable and unaffected by ChABC treatment. (**A**) Quantification of the total distance traveled during each OFT trial. Not significant; *n* = 12 Ctrl and 10 Chst11cKO mice. (**B**) Quantification of the total distance traveled in the EPM. Not significant; *n* = 10 Ctrl and 11 Chst11cKO mice. (**C**) Quantification of the total distance traveled by Ctrl and Chst11cKO mice in the OFT during each trial. Animals were injected with ChABC or Pen as a control. Not significant; *n* = 13, 13, 16, and 16 mice for the Ctrl Pen, Chst11cKO Pen, Ctrl ChABC, and Chst11cKO ChABC conditions, respectively. (**D**) Quantification of the total distance traveled by Ctrl and Chst11cKO mice in the EPM. Not significant; *n* = 13, 12, 13, and 14 mice for the Ctrl Pen, Chst11cKO Pen, Ctrl ChABC, and Chst11cKO ChABC conditions, respectively. All data are shown as the mean ± SEM.

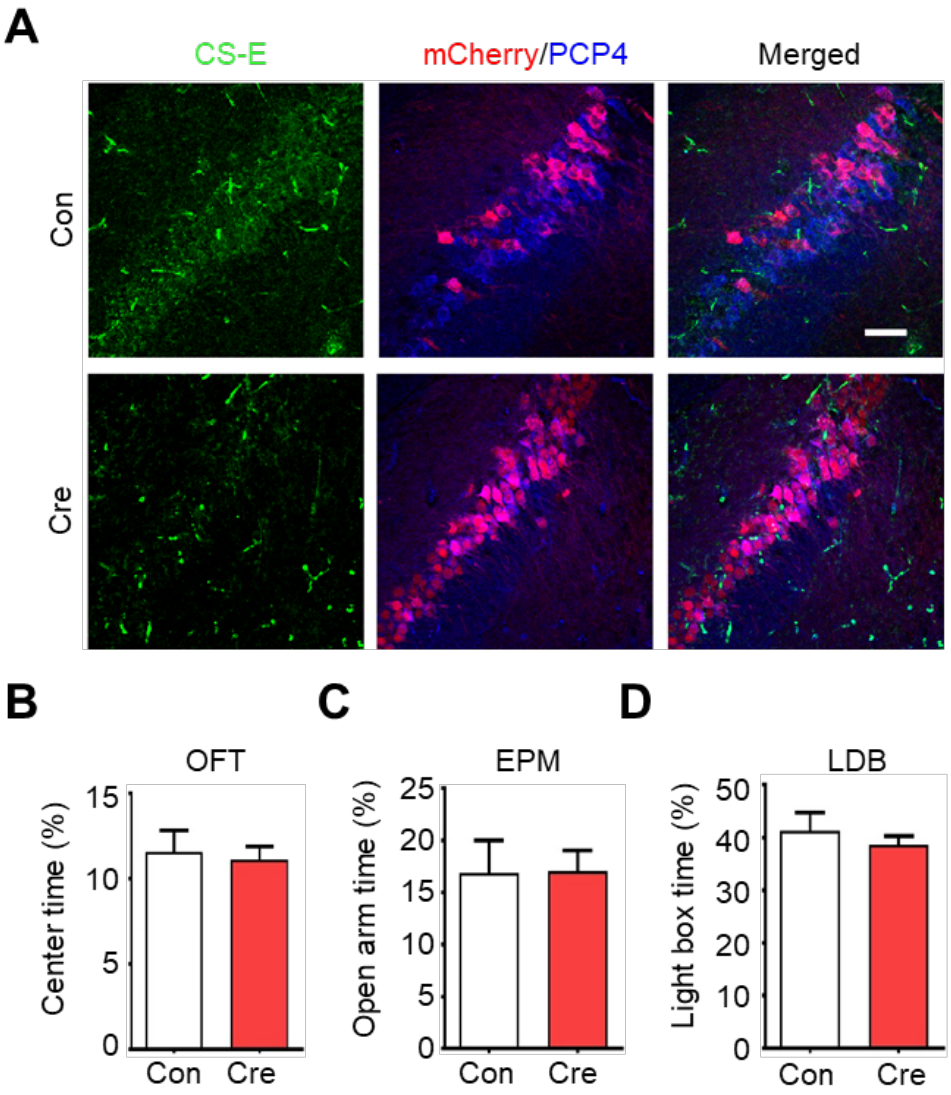

Figure S13. Specific deletion of 4-*O*-sulfation in CA2 pyramidal neurons does not affect anxiety-like behavior. (**A**) Reduced 4-*O*-sulfation in CA2 neurons infected with AAV-CaMKIIα-mCherry-Cre (Cre). Representative images showing the hippocampal CA2 regions of floxed *Chst11* mice injected with AAV-CamKIIα-mCherry (Con) or AAV-CaMKIIα-mCherry-Cre (Cre). Brain sections were labeled with an anti-PCP4 antibody (blue), anti-CS-E antibody (green), and mCherry (red). Scale bar, 50 μm. (**B** to **D**) Cre-injected animals did not exhibit changes in anxiety-like behavior. Percentage of time spent in the center of the arena during the OFT (**B**). Percentage of time spent in the open arms of the EPM (**C**). Percentage of time spent in the light box of the LDB (**D**). *n* = 10 pairs of Con- and Cre-injected mice for the OFT. *n* = 9 and 10 pairs of Con- and Cre-injected mice, respectively, for the EPM and LDB tests. All data are shown as the mean ± SEM.

Supplementary Materials and Methods

Animals

Chst11$^{loxP/loxP}$ and Chst11$^{+/-}$ mice were kindly provided by Prof. Melitta Schachner (Rutgers University) (1). Transgenic mice expressing the Cre recombinase under the control of the human nestin promoter (nestin-*Cre*$^{+/-}$) were purchased from Jackson Laboratory. Chst11$^{+/-}$; nestin-*Cre*$^{+/-}$ mice, generated by crossing Chst11$^{+/-}$ with nestin-*Cre*$^{+/-}$ mice, were crossed with Chst11$^{loxP/loxP}$ mice to generate double heterozygous nestin-*Cre*$^{+/-}$;Chst11$^{loxP/-}$ mice. These mice were then mated with Chst11$^{loxP/loxP}$ mice to establish animals for the experiments. The resulting nestin-*Cre*$^{-/-}$; Chst11$^{loxP/-}$ animals are Ctrl mice, and nestin-*Cre*$^{+/-}$; Chst11$^{loxP/-}$ are Chst11cKO mice, as indicated throughout the text. The Chst11cKO mice appeared normal, although they had slightly reduced birth rates (~2-6 embryos per pregnant mouse). Animals were maintained in the Animal Facility of the California Institute of Technology (Caltech). All animal procedures were performed in accordance with the NIH Guide for the Care and Use of Laboratory Animals and were approved by the Institutional Animal Care and Use Committee of Caltech.

Antibodies and chemicals

The following antibodies were used at the indicated dilutions: anti–PSD-95 (1:500, MA1-046) from Thermo Fisher Scientific; mouse anti-gephyrin (1:500, 147 011) from Synaptic Systems; rabbit anti-MAP2 (1:1000, AB5622) and rabbit anti-phospho-CREB (phospho-Ser133, 1:500-1000, 06-519) from Millipore; rabbit anti-CREB (48H2, 1:800, 9197S) from Cell Signaling Technologies; mouse anti-GFP (1:1000, A-11120) from Invitrogen; mouse anti-parvalbumin (1:500, SAB4200545) and rabbit anti-PCP4 (1:200, HPA005792) from Sigma-Aldrich. Fluorescein-labeled *Wisteria Floribunda* lectin (WFA, 1:300, FL-1351) was purchased from Vector Labs. The mouse anti-CS-E antibody was generated as previously described (2). Alexa Fluor® (AF) 488 dye-conjugated phalloidin was purchased from Thermo Fisher Scientific (A12379). Chemicals employed in this study include CS-A, -C, -E and -D polysaccharides (Seikagaku, Super Special Grade). ChABC (C3667) was purchased from Sigma-Aldrich. The sulfotransferase inhibitor (Inhib) was developed and synthesized by the Hsieh-Wilson laboratory (3).

Analysis of chondroitin sulfate disaccharide composition

Disaccharide analysis was performed as previously described (4). Cortical regions dissected from mouse brains were homogenized in ice-cold acetone and centrifuged at 4,000 xg. The precipitated, air-dried pellets were thoroughly digested with 2 mg/mL of pronase (Sigma-Aldrich) at 55 °C for 24 h. The pronase was then inactivated by heating to 80 °C for 20 min, followed by cooling for 15 min at −20 °C. After further digestion with DNase at 37 °C for 1 h, the mixture was centrifuged at 4000 rpm for 15 min. The supernatant was transferred and cooled on ice for 15 min. The proteins were precipitated with 10% (*wt/vol*) of cold trichloroacetic acid and incubated at 4 °C overnight. The acid-soluble fraction was extracted five times with diethyl ether (1:1, *vol/vol*). The remaining samples were then left to evaporate in a fume hood for 3 h and subsequently neutralized with 1 M Na_2CO_3. Glycosaminoglycans were precipitated with 5% sodium acetate in 75% ethanol overnight at −20 °C. After centrifugation at 4000 rpm for 15 min, the pellet was dissolved in water. An aliquot of the sample was digested with ChABC at 37 °C overnight. The digested glycans were derivatized with aminoacridone (0.1 M solution) and then analyzed by high-performance liquid chromatography (HPLC). Identification and quantification of the disaccharides was achieved by comparison with authentic, unsaturated disaccharide standards derived from natural CS (Seikagaku).

Neuronal cultures and chemical treatments

Primary hippocampal neuron cultures were prepared as previously described (5). Briefly, hippocampal tissues were dissected from E15 mouse embryos, and gentle dissociation of neuronal cells was achieved using a papain solution. Isolated neuronal cells were plated on poly-D,L-ornithine (PDL)-coated coverslips and cultured for 14–16 days in Neurobasal medium supplemented with B-27 (Gibco™, Thermo Fisher Scientific) and GlutaMAX™ (Invitrogen). Solutions of CS-A, CS-C, CS-D, or CS-E polysaccharides (20 µg/ml final concentration) were added to the culture medium 24 h before fixation of the neurons with 4% (*wt/vol*) of paraformaldehyde (PFA). ChABC was dissolved in phosphate-buffered saline (PBS) containing 0.01% bovine serum albumin (BSA), according to the manufacturer's instructions. ChABC was then

added to the culture medium at 0.05 U/ml, 2, 8 or 24 h before fixation of the neurons. PBS was used as a control. The sulfotransferase inhibitor (Inhib) was dissolved in DMSO before applying to the culture medium of neurons at a final concentration of 10 μM for 24 h. DMSO was used as a control.

Immunohistochemistry

After 14–16 days in vitro (DIV), cultured hippocampal neurons were fixed with 4% (*wt/vol*) PFA solution for 15 min. Neurons were then incubated with primary antibodies diluted in blocking buffer (5% *vol/vol* goat serum, 0.4% Triton X-100 in PBS, pH 7.4), overnight at 4 °C. After three washes with PBS, the neurons were incubated with AlexaFluor (AF)-conjugated secondary antibodies in blocking buffer at 22–25 °C for 1.5 h and washed three times with PBS. Immunohistochemistry of brain sections was performed as previously described (6). Briefly, mice were transcardially perfused with PBS followed by 4% PFA. Brains were dissected and post-fixed in 4% PFA at 4 °C overnight. Brains were then transferred to 15% sucrose, then 30% sucrose, in 0.1 M PBS (pH 7.4) each overnight and embedded in optimal cutting temperature (OCT) compound (SAKURA). Coronal sections (30 μm) were cut using a Leica CM1850 cryostat and stored in 30% ethylene glycol and 15% sucrose in PBS at −20 °C. Slices were stained with antibodies diluted in blocking buffer (5% *vol/vol* goat serum, 0.1% Triton X-100 in PBS, pH 7.4), overnight at 4 °C. Coverslips and slices were mounted with VECTASHIELD Mounting Medium (Vector Labs).

Viruses

AAV5-CamKIIα-mCherry and AAV5-CaMKIIα-mCherry-Cre were obtained from the Vector Core at the University of North Carolina at Chapel Hill. Vesicular stomatitis virus G (VSV-G) pseudotyped lentivirus expressing GFP was packaged in the Hsieh-Wilson laboratory.

Stereotaxic surgery

Viral delivery was performed as previously described (7). The VSV-G pseudotyped lentivirus expressing GFP was injected into the hippocampal CA1/CA2 regions (anteroposterior, −2.0 mm;

mediolateral, ±1.7 mm; dorsoventral, −1.5 mm; all coordinates relative to bregma) or CA3 region (anteroposterior, −1.7 mm; mediolateral, ±1.9 mm; dorsoventral, −1.9 mm; all coordinates relative to bregma). A 3-μl aliquot of lentivirus was injected bilaterally using a stereotaxic injector (Kopf Model 900). Four weeks after injection, brain sections from the lentivirus-infected mice were incubated with a GFP antibody overnight at 4 °C, followed by incubation with an Alexa Fluor® (AF) 488 dye-conjugated secondary antibody for 2 h at room temperature (RT). 4′,6-Diamidino-2-phenylindole (DAPI, Thermo Fisher, 1:3000) was added to the PBS wash buffer to stain for 10 min. Alternatively, 200 nl of either AAV5-CamKIIα-mCherry or AAV5-CaMKIIα-mCherry-Cre was injected bilaterally into the hippocampal CA2 regions of Chst11$^{loxp/loxp}$ mice (anteroposterior, −1.6 mm; mediolateral, ±1.6 mm; dorsoventral, −1.7 mm; all coordinates relative to bregma). Mice were subsequently subjected to a range of behavioral tests three weeks after surgery. ChABC injections were performed similarly. Briefly, 1 μl of ChABC or penicillinase (10 U/ml) was injected bilaterally into the hippocampal CA2 region. Injected mice were either euthanized for immunohistochemistry or subjected to behavioral tests, 2 weeks after surgery.

Image acquisition and quantification

All stained neuron and brain sections were imaged using a Zeiss 700 confocal microscope, with the investigator blind to the treatment or genotype. For PNN studies in cultured hippocampal neurons, at least five regions under the visual field were randomly imaged to represent the culture condition. Each image was captured throughout the entire depth of the region by z-stacking. Quantification of the cell numbers labeled by specific markers, such as WFA, was done manually. Quantification of the size and density of PSD-95 and gephyrin, as well as the density of p-CREB and total CREB, was performed using Image-J, as previously described (7). Briefly, for puncta analysis, three dendrites of each neuron were selected and cropped from the original image for analysis. The cropped images were color separated, and the channel of interest was analyzed after setting a fixed threshold for all the conditions. The readout was generated with the following two parameters: a) total count, with each unit corresponding to one puncta; and b) area, indicating the size of the puncta. The intensity analysis of p-CREB and total CREB was performed similarly, and

the total intensity of each single neuron was obtained after setting a threshold for the image. For dendritic spine analyses, we considered four different spine shapes, including filopodia, stubby, thin, and mushroom. Mushroom-shaped spines are considered mature and form stabilized synaptic connections (8). The density of mature spines was therefore calculated by dividing the number of dendritic spines with mushroom-shaped heads by the length of the dendrite. The head width of each protrusion and the length of each dendrite were measured, as well as the total number of protrusions on each dendrite.

Electrophysiology

Hippocampal slices were obtained from 5–7 week old Ctrl or Chst11cKO mice. After decapitation, mouse brains were extracted, trimmed, and 400-μm transverse hippocampal slices were cut on a vibratome (VT-1000s, Leica) in ice-cold sucrose-artificial cerebrospinal fluid (aCSF) solution (in mM: 213 sucrose, 2.5 KCl, 1.2 NaH_2PO_4, 25 $NaHCO_3$, 10 glucose, 7 $MgSO_4$, 1 $CaCl_2$, pH 7.3). Slices were then incubated in normal aCSF (in mM: 124 NaCl, 2.5 KCl, 1.2 NaH_2PO_4, 24 $NaHCO_3$, 25 glucose, 1 $MgSO_4$, 2 $CaCl_2$, bubbled with 95% O_2/5%CO_2) at 34.5 °C for 30 min, and then kept at RT until use. Whole-cell voltage clamp recordings were performed on pyramidal neurons in the CA2, identified based on their anatomical features. Electrical signals were filtered at 3 kHz with an Axon MultiClamp 700B (Molecular Devices) and collected at 20 kHz with an Axon Digidata 1550A (Molecular Devices). For miniature EPSCs recordings, pipette solution contained (in mM:145 $Cs(CH_3)SO_3$, 2 NaCl, 10 HEPES, 0.2 EGTA, 5 QX-314 bromide, 4 Mg-ATP, 0.3 Na-GTP, pH 7.25). Tetrodotoxin (TTX, 0.5 μM) and picrotoxin (PTX, 100 μM) were included in the aCSF. For miniature IPSCs recordings, pipette solution contained (in mM: 145 CsCl, 2 NaCl, 10 HEPES, 0.2 EGTA, 5 QX-314 bromide, 4 Mg-ATP, 0.3 Na-GTP, pH 7.25). TTX (0.5 μM), 6-cyano-7-nitroquinoxaline-2,3-dione (CNQX, 10 μM) and DL-2-amino-5-phosphonopentanoic acid (APV, 25 μM) were included in the aCSF.

Two-trial social memory test

Two-trial social memory experiments were performed as previously described (9). The subject mice were 2–3 months old male mice, and the stimulus mice were 4–6 weeks old male mice. At the beginning of the test, each subject mouse was singly housed in a cage similar to its home cage for 30 min. The lid of the cage was removed to allow filming of social activities. Each subject mouse was left in the cage to habituate for 30 min under dim lighting conditions. After habituation, a group-housed stimulus mouse was placed in each cage for the first interaction of 2 min. The stimulus mouse was removed after the first trial, then re-introduced to the same subject mice after 30 min. The second trial lasted another 2 min. All mice were then returned to their home cages and group housed. The test trials were videotaped and subsequently analyzed for the total interaction time between each subject mouse and the stimulus mouse.

Anxiety-related behavioral tests

Adult mice of both genders, aged 2–3 months, were used for all anxiety-related tests. The OFT were performed as previously described (6). Briefly, each mouse was placed in the lower left corner of a 50 × 50 cm white box, and activity was recorded for 10 min by a ceiling-mounted video camera. The total distance traveled and center entries were scored using EthoVision software. After each behavioral test, mice were returned immediately to their home cage.

The elevated plus maze (EPM) was performed as previously described (10). Briefly, mice were exposed for 5 min to an elevated plus maze (elevated 35 cm, arms 29 x 7.7 cm, closed arm walls 16.5 cm, center piece 7.7 x 7.7 cm, low light condition). Each mouse was placed in the central area of the maze with open access to any arm. The number of arm entries and the amount of time spent in the open and closed arms were recorded for subsequent scoring, using video tracking systems. The elevated plus maze was cleaned with water and disinfectant (NPD®) between mice.

For the light-dark box test (LDB), each mouse was initially placed in the dark compartment of the light-dark box (lit chamber 30 x 25.5 cm, dark chamber 15 x 25.5 cm, height 30 cm, opening 5 x 5 cm, bright light condition). The movements of the mouse inside the box were recorded for 10 min to assess bright space anxiety. Before and after each experimental trial, the surfaces of the training and testing boxes are cleaned with water and disinfectant (NPD®).

Statistical analyses

All experimental and data analysis in this work were conducted blinded, including the immunohistochemistry, electrophysiology and behavioral tests. The number of replicates (n) is indicated in each figure legend and all experiments were performed at least in triplicate independently unless otherwise indicated. Data are expressed as the mean ± SEM. The unpaired, two-sided Student's *t* test or one-way and two-way analysis of variance (ANOVA) was used followed by Tukey's multiple comparisons to evaluate the significance of differences between two experimental conditions and three or more experimental conditions, respectively. Non-normally distributed data were analyzed by Wilcoxon rank-sum test. The Kolmogorov–Smirnov test was used to study cumulative distribution functions. The level of significance was set at $^{*}P < 0.05$, $^{**}P < 0.01$, $^{***}P < 0.001$, $^{****}P < 0.0001$.

SI References

1. S. Bian *et al.*, Dermatan sulfotransferase Chst14/D4st1, but not chondroitin sulfotransferase Chst11/C4st1, regulates proliferation and neurogenesis of neural progenitor cells. *J. Cell Sci.* **124**, 4051-4063 (2011).
2. J. M. Brown *et al.*, A sulfated carbohydrate epitope inhibits axon regeneration after injury. *Proc. Natl. Acad. Sci. U.S.A.* **109**, 4768-4773 (2012).
3. S. T. Cheung *et al.*, Discovery of a small-molecule modulator of glycosaminoglycan sulfation. *ACS Chem. Biol.* **12**, 3126-3133 (2017).
4. S. Miyata, Y. Komatsu, Y. Yoshimura, C. Taya, H. Kitagawa, Persistent cortical plasticity by upregulation of chondroitin 6-sulfation. *Nat. Neurosci.* **15**, 414-422, s411-412 (2012).
5. J. E. Rexach *et al.*, Dynamic O-GlcNAc modification regulates CREB-mediated gene expression and memory formation. *Nat. Chem. Biol.* **8**, 253-261 (2012).
6. A. C. Wang, E. H. Jensen, J. E. Rexach, H. V. Vinters, L. C. Hsieh-Wilson, Loss of O-GlcNAc glycosylation in forebrain excitatory neurons induces neurodegeneration. *Proc. Natl. Acad. Sci. U.S.A.* **113**, 15120-15125 (2016).
7. H. Huang *et al.*, Cdk5-dependent phosphorylation of liprinα1 mediates neuronal activity-dependent synapse development. *Proc. Natl. Acad. Sci. U.S.A.* **114**, E6992-E7001 (2017).
8. N. L. Rochefort, A. Konnerth, Dendritic spines: from structure to in vivo function. *EMBO Rep.* **13**, 699-708 (2012).
9. F. Leroy, D. H. Brann, T. Meira, S. A. Siegelbaum, Input-timing-dependent plasticity in the hippocampal CA2 region and its potential role in social memory. *Neuron* **102**, 260-262 (2019).

10. A. A. Walf, C. A. Frye, The use of the elevated plus maze as an assay of anxiety-related behavior in rodents. *Nat. Protoc.* **2**, 322-328 (2007).